

# SYNTHESIS, CHARACTERIZATION AND GAS SENSING PROPERTIES OF BINARY OXIDE $\text{In}_2\text{O}_3$ : $\text{MoO}_3$ THIN FILMS .

<sup>1</sup>Kothawade N B, , <sup>2</sup>Dhanwate S. V.

<sup>1</sup>Associate Professor and Head Department of Physics, Arts ,Commerce and Science College,  
Kalwan (Manur) Dist. Nashik, India- 423501

<sup>2</sup>Associate Professor and Head Department of Physics, Swami Muktanand College of Science ,  
Yeola ( Nashik), India -423401

## ABSTRACT

$\text{In}_2\text{O}_3$  doped  $\text{In}_2\text{O}_3$ : $\text{MoO}_3$  binary oxide thin films were prepared by using spray pyrolysis technique on glass substrate for various concentration at  $400^\circ\text{C}$  temperature . the effect of  $\text{In}_2\text{O}_3$

On structural , morphological and electrical properties have been studied . thin films were characterized using X-ray diffraction (XRD), SEM and Electrical properties. The obtained film shows good crystalline in nature . the average grain size estimated is 11 nm the other properties were under consideration The sensitivity and selectivity of sensor can be improved by dopants or additives which can change the gas sensing characteristics. Nano composite term contain mixture of two or more nano oxide materials like binary oxide.. . Nano composite films consists of Nano crystalline or amorphous phase of a least two different materials  $\text{In}_2\text{O}_3$  as dopant and  $\text{MoO}_3$  as a functional material in film. The precursor  $\text{InCl}_3$  and  $\text{MoCl}_5$  of concentrations 0.2N:0.1N.

**KEYWORDS** :- , XRD , SEM EDS, Electrical, Gas sensor, spray pyrolysis technique , binary oxide thin films, $\text{In}_2\text{O}_3$  ,  $\text{MoO}_3$ ,Thin film.

## INTRODUCTION

Nanocomposite is mixture of two or more nano oxide materials like binary oxide, ternary oxide . Indium oxide ( $\text{In}_2\text{O}_3$ ) is an n-type semiconducting chemiresistive oxide sensor material with a direct band gap of 3.55–3.75 eV, has been reported as the best potential gas sensing material due to its good conductivity and high stability. Indium oxide has been produced in different forms of nanostructures, such as nanowires, nanospheres, nanorods, nanoporous and nanofibers, showing interesting gas sensing capabilities for various gases including nitric oxide, methane, ammonia, acetone and ethanol. Dopant element into  $\text{In}_2\text{O}_3$  sensing materials may cause

the change of crystalline structure and grain size as well as impurity levels and surface defects, which can significantly improve the gas sensing performances of  $\text{In}_2\text{O}_3$  gas sensor.

Molybdenum oxide is a wide band gap n- type semiconductor with band gap energy of 2.39-2.9 eV.  $\text{MoO}_3$  exhibits the highest value of work function among the non-soluble transition metal oxides.  $\text{MoO}_3$  nanoparticles have attracted a great deal of attention due to their unique physical and chemical properties that differ from those in the bulk, in particular for their high surface-to-volume ratio. In the transition metal oxides  $\text{MoO}_3$  is found to be a suitable candidate for many technological applications such as electrochromic display devices, gas sensors, optical memories and lithium batteries.

## EXPERIMENTAL METHODS

Binary oxide  $\text{In}_2\text{O}_3$ :  $\text{MoO}_3$  thin films were prepared by spray pyrolysis technique on glass substrate. The spray Pyrolysis process was carried out at substrate temperature  $400^\circ\text{C}$ . The precursor  $\text{InCl}_3$  and  $\text{MoCl}_5$  of concentrations 0.1N, 0.2N and 0.3N were used, designed and assembled in laboratory to overcome limitations of conventionally designed setup; such as number of optimized parameters, reliability and homogeneity of the deposited films. The thin films of  $\text{In}_2\text{O}_3$ :  $\text{MoO}_3$  were prepared for concentration in proportion of 0.2N:0.1N. The study of characteristics such as SEM, EDS, XRD, resistivity, activation energy, TCR and gas sensing property were done to study the changes due to dopant.

## RESULTS AND DISCUSSION

### X-RAY DIFFRACTION ANALYSIS (XRD)

Figure shows XRD pattern of binary oxide  $\text{In}_2\text{O}_3$ :  $\text{MoO}_3$  thin films on glass substrate fired at  $400^\circ\text{C}$  of the peak position values of the  $20-80^\circ$  range using X powder  $12(\text{CuK}\alpha)$  Radiation.

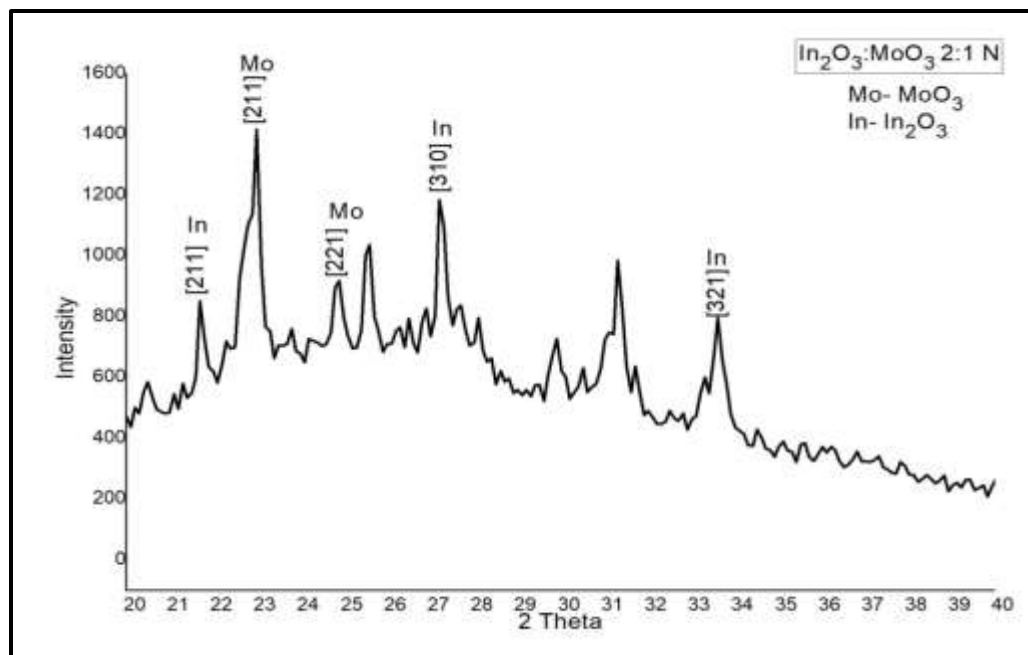


**Figure:** XRD of Binary oxide  $\text{In}_2\text{O}_3$ :  $\text{MoO}_3$  thin film with concentration 0.2N:0.1N

XRD of Binary oxide  $\text{In}_2\text{O}_3$ :  $\text{MoO}_3$  thin film with concentration 0.2N:0.1N is shown in table

Plane (hkl)	2 $\theta$	d-spacing	Intensity	I/I <sub>o</sub>	FWHM
In- 211	21.72	4.09424	801	67.3	1.912
Mo-211	23.01	3.86105	1190	100	0.812
Mo-211	24.74	3.5955	579	48.7	4.285
In- 310	27.21	3.27363	1020	85.7	0.808
In- 321	33.60	2.66577	796	56.2	3.399

The average grain size was determined by using Debye-Scherrer formula,

$$D = 0.9\lambda / \beta \cos\theta$$

$\beta$  is full angular width of diffraction peak at half maximum peak intensity,  $\lambda$  is wavelength of X-radiation.

As per structural analysis the grain size were calculated by using Scherrer formula. The grain size of film at concentrations 0.2N:0.1N, were found 11 nm.

### SCANNING ELECTRON MICROSCOPY (SEM)

Figure shows that the SEM of binary oxide  $\text{In}_2\text{O}_3:\text{MoO}_3$  thin films of 0.2N: 0.1N was deposited on glass substrate using a Spray Pyrolysis Technique and fired at  $400^\circ\text{C}$ . The magnifications of all SEM images are taken at 10000X.

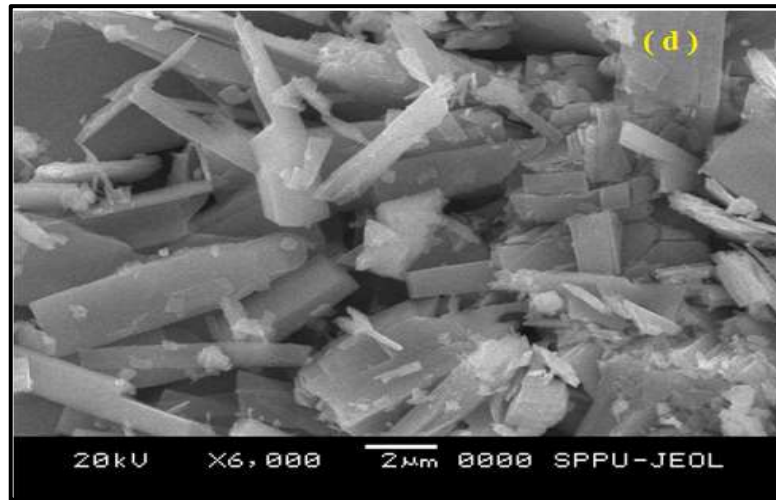


**Figure :** SEM of Binary oxide  $\text{In}_2\text{O}_3:\text{MoO}_3$  thin with concentration 0.2N:0.1N

Binary oxide  $\text{In}_2\text{O}_3:\text{MoO}_3$  Films prepared by Spray Pyrolysis were observed to be non porous as per SEM analysis. As per SEM analysis, the average particle size of film was calculated by using image j software. The average particle size of film at concentrations 0.2N:0.1N was found as 198 nm.

The specific surface area of Binary oxide  $\text{In}_2\text{O}_3:\text{MoO}_3$  thin film was calculated using BET method for spherical particles using the equation ,

$$S_w = \frac{6}{\rho d}$$

Where,  $d$  is the diameter of the particles,  $\rho$  is the density of the particles.

The specific Surface area with different concentrations of binary oxide  $\text{In}_2\text{O}_3$ :  $\text{MoO}_3$  was found as  $26.49002 \text{ m}^2/\text{g}$ .

### ENERGY DISPERSIVE X-RAY ANALYSIS (EDS)

Figure shows that the count (along Y- axis) Verses KeV (along X-axis) EDS of 0.2N:0.1N concentration of binary oxide  $\text{In}_2\text{O}_3$ :  $\text{MoO}_3$  thin films.

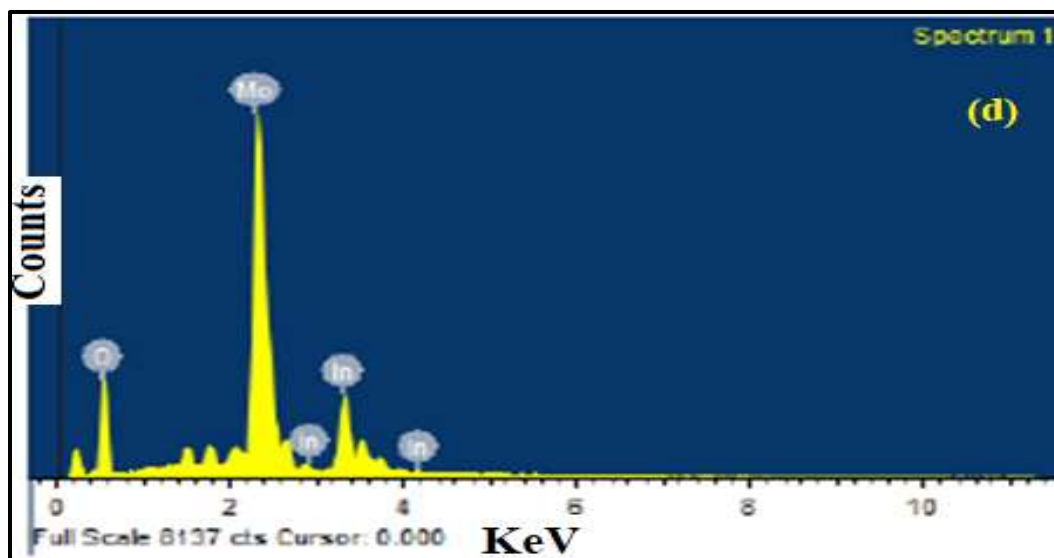


**Figure :** EDS of Binary oxide  $\text{In}_2\text{O}_3$ :  $\text{MoO}_3$  thin film with concentration 0.2N:0.1N

From the EDAX spectra, it is found that mass% and at. wt.% of In, Mo and O is nearly matched.

EDS of Binary oxide  $\text{In}_2\text{O}_3$ :  $\text{MoO}_3$  thin film with Concentration 0.2N:0.1N is shown in table

Element	Atomic %
O	85.48
Mo	11.44
In	3.08

## ELECTRICAL CHARACTERIZATION

The electrical characterization was done to measure the variation in electrical resistance at operating temperatures in air atmosphere, the resistivity, TCR and activation energy.

### RESISTIVITY

The DC resistance of In<sub>2</sub>O<sub>3</sub>:MoO<sub>3</sub> thin films with normality 0.2N:0.1N on glass substrate and fired at 400<sup>0</sup>C was measured by using half bridge method as a function of temperature. Figure shows resistance variation of In<sub>2</sub>O<sub>3</sub>:MoO<sub>3</sub> thin films with normality 0.2N:0.1N temperature variation in an atmosphere. There is decrease in resistance with increase in temperature indicating semiconductor behavior, obeying  $R = R_0 e^{-\Delta E/KT}$  in the temperature range of 40-350<sup>0</sup>C.

The resistance In<sub>2</sub>O<sub>3</sub>:MoO<sub>3</sub> thin films with normality 0.2N:0.1N falls rapidly, decreases linearly up to certain transition temperature and after resistance decreases exponentially with increase in temperature and lastly saturates to steady level.

The resistivity of In<sub>2</sub>O<sub>3</sub>:MoO<sub>3</sub> thin films at constant temperature is calculated using the relation,

$$\rho = (R \times A) / l$$

$$\rho = (R \times b \times t) / l \quad \text{ohm-m}$$

Where,  $R$  = Resistance of In<sub>2</sub>O<sub>3</sub>:MoO<sub>3</sub> thin film at constant temperature

$t$  = thickness of the film sample

$l$  = length of the thin film

$b$  = breadth of the thin film

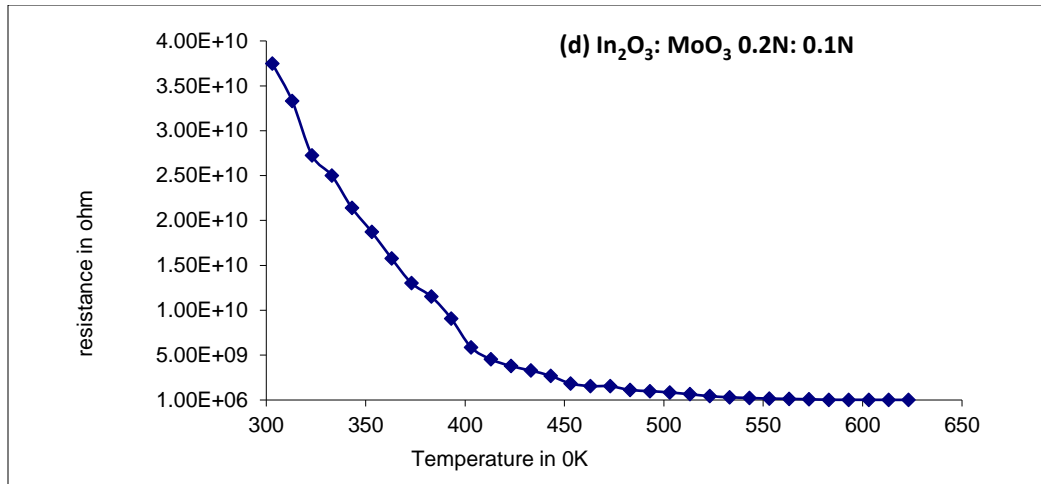


**Figure:** Resistance of Binary oxide  $\text{In}_2\text{O}_3$ :  $\text{MoO}_3$  thin with concentration 0.2N:0.1N

The resistivity of binary oxide  $\text{In}_2\text{O}_3$ : $\text{MoO}_3$  sample with concentrations 0.2N:0.1N, of  $\text{MoO}_3$  as additives in  $\text{TiO}_2$  film was calculated  $14.980 \times 10^3 \Omega\text{-m}$ .

### ACTIVATION ENERGY

Figure shows plot of  $\log(R)$  versus reciprocal of temperature,  $(1/T)$  for  $\text{In}_2\text{O}_3$ : $\text{MoO}_3$  thin films with normality 0.2N:0.1N.

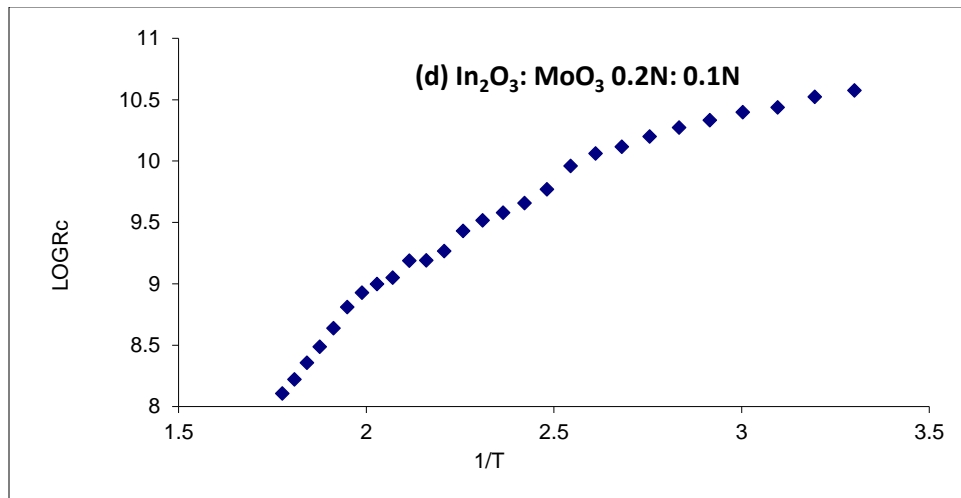


**Figure:** Activation energy of Binary oxide  $\text{In}_2\text{O}_3$ : $\text{MoO}_3$  thin film with concentration 0.2N:0.1N

This plot is reversible in both heating and cooling cycles obeying the Arrhenius equation

$$R=R_0 e^{-\Delta E/KT}$$

Where,  $R_0$  = the constant = Resistance at room temperature

$\Delta E$  = The activation energy of the electron transport in the conduction band,

$K$  = Boltzman constant and

$T$  = Absolute temperature

The Activation energy at high temperature and at low temperature were found 0.1707eV and 0.7976 eV respectively at 0.2N:0.1N .

### TEMPERATURE COEFFICIENT OF RESISTANCE (TCR)

Temperature coefficient of resistance (TCR) of  $\text{In}_2\text{O}_3$ :  $\text{MoO}_3$  thin films prepared at  $400^\circ\text{C}$  is calculated by using the following relation,

$$TCR = \frac{1}{R_0} \left( \frac{\Delta R}{\Delta T} \right) / ^\circ K$$

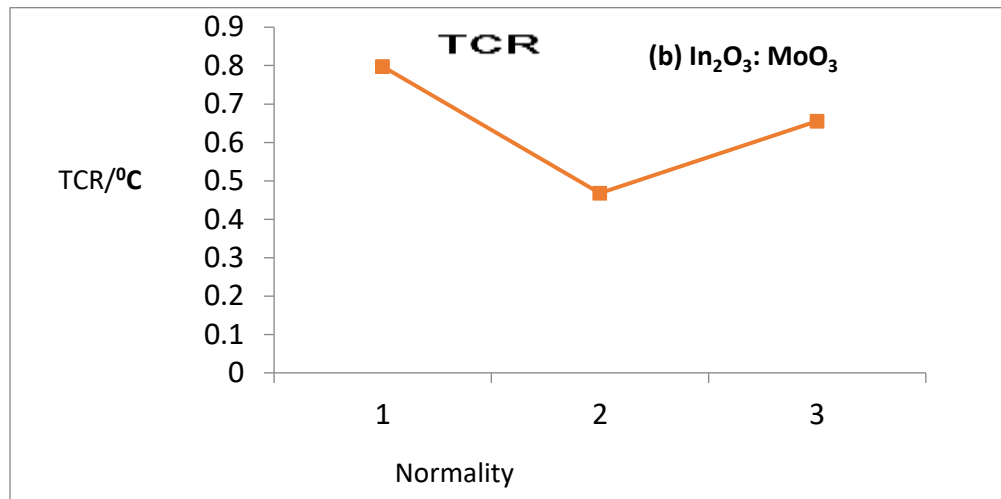


**Figure:** TCR graph of binary oxide  $\text{In}_2\text{O}_3$ :  $\text{MoO}_3$  thin film with concentration 0.2N:0.1N

The temperature coefficient of resistance (TCR) was found as  $0.0179 / ^\circ C$  .



## GAS SENSING PROPERTIES

The main characterization is the optimization of operating temperature of film sample for test gases. On the basis of measured data, the sensitivity and selectivity of thin film sensor for a fixed gas concentration of 1000 ppm in air surrounding condition are estimated.

The variation in sensitivity of binary oxide  $\text{In}_2\text{O}_3:\text{MoO}_3$  thin films as a function of temperature and for LPG, Ethanol,  $\text{NH}_3$ , CO and  $\text{NO}_2$  gases [1000 ppm concentration]. The operating temperature was varied at the interval of  $50^\circ\text{C}$ . From the measured resistance in air as well as in gas atmosphere, the sensitivity of gas was determined at particular operating temperature using the following equation ,

$$\text{Sensitivity}(S) = \left| \frac{R_a - R_g}{R_a} \right| \times 100$$

Where,

$R_a$  – resistance of thin film in air atmosphere,

$R_g$  – resistance of thin film in gaseous atmosphere.

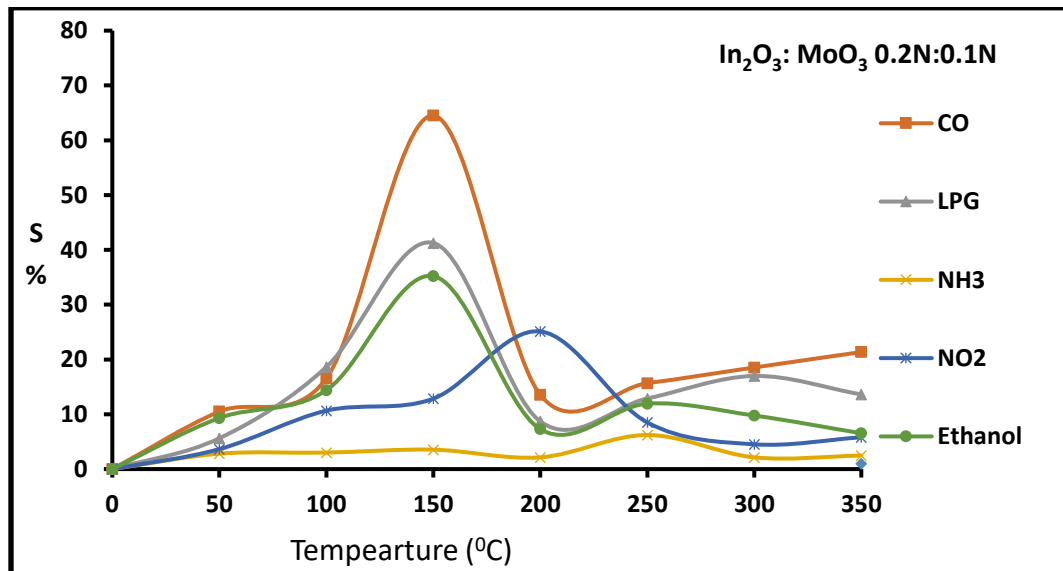


**Figure:** Gas sensitivity response of Binary oxide  $\text{In}_2\text{O}_3 : \text{MoO}_3$  thin film with concentration 0.2N:0.1N

The film of binary oxide  $\text{In}_2\text{O}_3:\text{MoO}_3$  was exposed to various gases. The film of binary oxide  $\text{In}_2\text{O}_3:\text{MoO}_3$  was exposed to various gases. The film of  $\text{In}_2\text{O}_3:\text{MoO}_3$  at 0.2N:0.1N showed 64.50% sensitivity for CO gas at operating temperature  $150^\circ\text{C}$  and CO gas concentration was at 300 ppm.

## CONCLUSION

The Binary oxide  $\text{In}_2\text{O}_3:\text{MoO}_3$  Nano crystalline thin films have been grown successfully on to glass substrate. The average particle size of film at concentrations 0.2N:0.1N was found 198 nm. Specific Surface area with different concentrations of binary oxide  $\text{In}_2\text{O}_3:\text{MoO}_3$  was found as  $26.49002\text{ m}^2/\text{g}$ . The atomic % of O, Mo, In were found as 85.48% ,11.44% and 3.08 % respectively. XRD gives the grain size of film 11 nm. The resistivity of sample was calculated  $14.980 \times 10^3\ \Omega\text{-m}$ . The Activation energy at high temperature and at low temperature were found as 0.1707eV and 0.7976 eV respectively. The temperature coefficient of resistance were found was  $0.0179/^\circ\text{C}$ . The film of  $\text{In}_2\text{O}_3:\text{MoO}_3$  at 0.2N:0.1N showed 64.50 % sensitivity for CO gas at operating temperature  $150^\circ\text{C}$  and CO gas concentration was at 300 ppm.

## REFERENCES

1. S. Basu, A. Dutta, Materials Chemistry and Physics 47(1997) 93-96
2. G. Uozumi, M. Miyayama, H. Yanagida, Journal of Materials Science 32 (11) (1997) 2991-2996.
3. Sian.T.S and Reddy.G.B, Appl.Surf.Sci., 2004,236, 1-5.
4. W. W. Chen, Y. K. Liu, Z. J. Qin, Y.
5. X. Chen, S.S. Mao, Chem. Rev. 107 (2007) 2891–2959.
6. Y.F. Sun, S.B. Liu, F.L. Meng, J.Y. Liu, L.T. Kong, J.H. Liu, Sensors 12 (2012) 2610–2631.
7. S. Matsushima, Y. Teraoka, N. Miura, N. Yamazoe, Jpn.J.Appl.Phys.27 (1988) 1798- 1802
8. J. G. Duh, J. W. Jou, B. S. Chiou, Electrochem.Soc.136 (1989) 2740-2747
9. P. Prathap, N. Revathi, K. T. R. Reddy, and R. W. Miles, Thin Solid Films 518, 1271 (2009).
10. T. Brezesnski, J. Wang, S. H. Tolbert and B. Dunn, Nat. Mater., 9 (2010) 146.

11. D. V. Ahire, S. D. Shinde, G. E. Patil, K. K. Thakur, V. B. Gaikwad, V. G. Wagh1 and G. H. Jain, International Journal On Smart Sensing And Intelligent Systems, Vol. 5, No. 3, September 2012,Issn 1178-5608.
12. E. B. Santos, F. A. Sigoli, I. O. Mazali, J. Solid State Chem. 190 (2012) 80-84.
13. Granqvist.C.G, Handbook of Inorganic Electrochromic Materials, Elsevier, 115.
14. Sian.T.S and Reddy.G.B, Appl.Surf.Sci., 2004,236, 1-5.
15. X. Chen, S.S. Mao, Chem. Rev. 107 (2007) 2891–2959.
16. Y.F. Sun, S.B. Liu, F.L. Meng, J.Y. Liu, L.T. Kong, J.H. Liu, Sensors 12 (2012) 2610–2631.
17. L.Gao, Li, Q., Song, Z., Wang Sens. Actuators B71 (2000) 179-183
18. S. Cho, J. Korean Phys. Soc. 60, 2058 (2012).
19. D.R. Patil, L.A.Patil, Sensors and Actuators B 123 (2007) 546–553.
20. L. Satyanarayana, K. Madhusudan Reddy, S.V. Manorama, Sensors and Actuators B 89(2003) 62-67.
21. D.M. Smyth, Solid State 129 (2000) 5–12.
22. Titkov.IE, Delimova.LA, Zubrilov.AS, Seredova.NV, Liniichuk.IA and GrekhovIV: J Mod Opt., 2009, 56, 653–660.
23. G. Korotcenkov, Sens. Actuators B: chem., 107, 2005, 209–232.
24. S. Matsushima, Y. Teraoka, N. Miura, N. Yamazoe, Jpn.J.Appl.Phys.27 (1988) 1798- 1802
25. J. G. Duh, J. W. Jou, B. S. Chiou, Electrochem.Soc.136 (1989) 2740-2747
26. S. Basu, A. Dutta, Materials Chemistry and Physics 47(1997) 93-96.
27. X. P. Shen, L. J. Guo, G. X. Zhu, C. Y. Xi, Z. Y. Ji and H. Zhou, RSC Adv., 2015, 5, 64228–64234.
28. X. Y. Lai, P. Li, T. L. Yang, J. C. Tu and P. Xue, Scr. Mater., 2012, 67, 293–296.